HHS Public Access

Author manuscript

Arthritis Rheumatol. Author manuscript; available in PMC 2023 July 01.

Published in final edited form as:

Arthritis Rheumatol. 2022 July ; 74(7): 1139–1146. doi:10.1002/art.42093.

The prominent role of hematopoietic peptidyl arginine deiminase 4 in arthritis: collagen and G-CSF induced arthritis model in C57BL/6 mice

Shoichi Fukui, MD, PhD[1,2], **Sarah Gutch**[1], **Saeko Fukui, MD**[1], **Deya Cherpokova, PhD**[1,2], **Karen Aymonnier, PhD**[1,2], **Casey E Sheehy**[1], **Long Chu**[1], **Denisa D Wagner, PhD**[1,2,3,*]

[1]Program in Cellular and Molecular Medicine, Boston Children's Hospital, Boston, MA 02115, USA.

[2]Department of Pediatrics, Harvard Medical School, Boston, MA 02115, USA.

[3]Division of Hematology/Oncology, Boston Children's Hospital, Boston, MA 02125, USA.

Abstract

Objectives—Genome-wide association studies have connected *PADI4*, encoding peptidylarginine deiminase 4 (PAD4), with rheumatoid arthritis (RA). PAD4 promotes neutrophil extracellular trap (NET) formation. We studied *Padi4* origin and NETs in an arthritis model in C57BL/6 mice.

Methods—To permit the effective use of C57BL/6 mice in the collagen-induced arthritis (CIA) model, we introduced the administration of granulocyte colony-stimulating factor (G-CSF) for four consecutive days in conjunction with the booster immunization on day 21. The model evaluated global ($Padi4^{-/-}$) and hematopoietic lineage-specific ($Padi4^{Vav1Cre/+}$) *Padi4*-deficient mice.

Results—G-CSF significantly increased the incidence and severity of arthritis in CIA. G-CSF-treated mice showed elevated citrullinated histone H3 (H3Cit) in plasma while vehicle-treated mice did not. Immunofluorescent microscopy revealed deposition of H3Cit in synovial tissue in G-CSF-treated mice. $Padi4^{-/-}$ mice developed less arthritis, demonstrating lower serum interleukin 6 and plasma H3Cit, less citrullinated histone H4 in synovial tissue, and less bone erosion observed by micro-computed tomography than $Padi4^{+/+}$ mice in the G-CSF-modified CIA model. Similarly, $Padi4^{Vav1Cre/+}$ mice developed less arthritis compared with $Padi4^{fl/fl}$ mice, and presented the same phenotype as $Padi4^{-/-}$ mice.

Conclusions—We succeeded in developing an arthritis model suitable for use in C57BL/6 mice that was fully compliant with high animal welfare standards. We observed an over 90% incidence

*Correspondence: denisa.wagner@childrens.harvard.edu (D.D.W.).

Contributors

Design of the study: ShF and DDW.

Experiments and acquisition of data: ShF, SG, SaF, KA, CES, DC, LC.

Interpretation of data: ShF and DDW.

Manuscript preparation: ShF and DDW.

Competing interests

Authors declare no conflict of interest on this research.

of arthritis in male mice and detectable NET markers. This model, with some futures consistent with human RA, demonstrates that hematopoietic PAD4 is an important contributor to arthritis development and may prove useful in future RA research.

Keywords

Rheumatoid Arthritis; Synovitis; Anti-Citrullinated Protein Antibodies; Neutrophil extracellular traps; Citrullinated histones

Rheumatoid arthritis (RA) is a chronic systemic inflammatory autoimmune disorder characterized by persistent joint inflammation resulting in cartilage and bone damage, disability, and systemic complications. One hallmark of RA is the presence of autoantibodies to citrullinated proteins. Genome wide association study (GWAS) on RA patients demonstrated an association with *PADI4* encoding peptidylarginine deiminase 4 (PAD4). (1)

PAD4, an enzyme that converts positively charged arginine to neutral citrulline and thus modifies immunological epitopes and protein function. PAD4 plays a role in releasing neutrophil extracellular traps (NETs) by citrullinating histones, which leads to the decondensation of chromatin. (2)

Padi4 deficiency alleviates arthritis and autoantibody production in inflammatory arthritis induced in tumor necrosis factor α-overexpressing mice, (3) collagen-induced arthritis (CIA) in DBA/1 mice, (4) and glucose-6-phosphate isomerase-induced arthritis in DBA/1 mice. (5) However, *Padi4* deficient mice in the K/BxN serum transfer arthritis model showed an absence of NETs, but did not demonstrate the amelioration of arthritis *in vivo*. (6) These inconsistent results suggest the effect of *Padi4* may depend on particular the murine model, more specifically whether NET-dependent or NET-independent pathways are essential. Thus, further evaluation of the contribution of *Padi4* to a murine arthritis is needed in a manner that meets current animal welfare criteria.

We hypothesized that the effects of *Padi4* observed in the CIA murine arthritis model are dependent on NETs, and more specifically hematopoietic cell-associated *Padi4.* Because we had *Padi4*-deficient mice on a C57BL/6 background, we aimed to induce arthritis using the collagen-induced arthritis (CIA) model in that strain. However, the susceptibility to CIA is linked to specific MHC class II genes (7) and C57BL/6 is not a highly susceptible strain for CIA. Despite attempts to improve the protocol, CIA in C57BL/6 mice is associated with a lower disease incidence and severity and more variability than seen in more susceptible strains such as DBA/1. (8) Additionally, concerns of animal welfare, including pain and distress in mice, made it impossible for us to use the original CIA protocol. (9) Specifically, the use of complete Freund's adjuvant (CFA) including heat-killed *Mycobacterium tuberculosis* in the booster immunization is not allowed in most institutions. (7) Therefore, we sought to develop a novel murine arthritis model on C57BL/6 background to address our hypothesis using two strains of genetically-engineered mice.

MATERIALS AND METHODS

Animals

Wild type C57BL/6 mice were bred in-house. *Padi4*$^{-/-}$ mice were originally generated by Y. Wang (10) and back-crossed with C57BL/6J. They were bred in-house and littermates derived from heterozygous-by-heterozygous crosses. *Padi4*$^{fl/fl}$ mice (stock no: 026708), previously described by Hemmers et al. (11), and *Vav1-iCre* mice (stock no: 008610) were purchased from Jackson Laboratory and intercrossed to generate mice lacking *Padi4* in the hematopoietic lineage (*Padi4*$^{Vav1Cre/+}$) following a female Cre + (carrier) and male Cre – (non-carrier) breeding strategy recommended by Joseph et al. (12) The abrogated *Padi4* expression in *Padi4*$^{Vav1Cre/+}$neutrophils was confirmed in our previous study. (13) All mice were housed in the animal facility of Boston Children's Hospital and were kept free from specific pathogens. Experimental protocols were approved by the Institutional Animal Care and Use Committee of Boston Children's Hospital (Protocol number: 20-01-4096R).

Collagen-induced arthritis and evaluation of arthritis

Male mice aged 8- to 12-weeks-old were immunized with the emulsion of complete Freund's adjuvant (CFA, catalog number: 7023, Chondrex, Redmond, WA) and 100μg of chicken type II collagen (CII, catalog number: 20012, Chondrex) in a 1:1 mixture (total 100μl) intradermally into the base of the tail on day 0. The booster immunization of CII with incomplete Freund's adjuvant (catalog number: 7002, Chondrex) was performed intrademally in a site proximal to the first injection site on day 21. The severity of arthritis was evaluated using the following clinical scoring system for each limb: 0, normal; 1, swelling in one finger joint; 2, swelling in more than one finger joint or wrist or ankle joint; 3, swelling in the entire paw; and 4, deformity and or ankylosis. The maximum score was 16 per mouse. Two evaluators (one knew the group allocation, the other did not) independently scored arthritis and arrived at agreements on final scorings.

Administration of granulocyte-colony stimulating factor (G-CSF)

Recombinant human G-CSF (Filgrastim, Neupogen®, Amgen, Inc., Thousand Oaks, CA) was injected at 10 μg peritoneally once daily from day 20 to day 23. Sterile saline was used as the vehicle control.

Immunofluorescence microscopy

The sections were fixed in zinc fixative (100 mmol/L Tris-HCl, 37 mmol/L zinc chloride, 23 mmol/L zinc acetate, 3.2 mmol/L calcium acetate), permeabilized with 0.1% Triton-X and 0.1% sodium citrate for 10 minutes at 4°C, blocked with 3% BSA in PBS with 0.05% Tween-20 at room temperature for an hour, and incubated with primary antibodies against H3Cit (1:1,000, catalog number: ab5103, Abcam, Cambridge, MA), Ly6G (1:500, catalog number: 551459, BD Pharmingen, San Jose, CA), at 4°C overnight. After washes, the sections were incubated with appropriate Alexa Fluor-conjugated secondary antibodies (1:1,500, catalog number: A-21206 (anti-Rabbit, Alexa Fluor 488) and A-21434 (anti-Rat, Alexa Fluor 555), Life Technologies, Carlsbad, CA) for 2 hours at room temperature. Hoechst 33342 (1:10,000, catalog number: H3570, Invitrogen) was

used to counterstain DNA. Images were obtained with a Zeiss Axiovert 200M wide-field fluorescence microscope (Zeiss, Oberkochen, Germany) with the Zeiss AxioVision software.

Statistics

Data were described with the median and interquartile range (IQR) for quantitative variables. We assessed the association between variables using Wilcoxon rank-sum test for quantitative variables. For the evaluation of the changes of plasma dsDNA and H3Cit, we used Wilcoxon signed rank test. The cumulative incidence of arthritis was estimated with the Kaplan-Meier method and log-rank test. The Bonferroni correction was used for the multiple comparison. All tests were two-sided, and a p-value < 0.05 was considered significant. All statistical analyses were performed using GraphPad Prism ver. 7.0 (GraphPad Software, San Diego, CA, USA).

See supplementary description on enzyme-linked immunosorbent assay (ELISA), double-stranded DNA measurement, micro-computed tomography (Micro-CT), histological evaluation, and immunoblotting.

RESULTS

We tested the CIA model on C57BL/6 mice. In the original protocol, the collagen-induced arthritis model needed two injections of the emulsion of type II collagen (CII) and complete Freund's adjuvant (CFA) on C57BL/6 mice. (9) However, the use of the second injection of CFA is not allowed in most institutions (7) including Boston Children's Hospital because of the pain and distress to mice. Therefore, we used one injection of the CII with CFA on day 0 and one injection of the CII with incomplete Freund's adjuvant on day 21 (Figure 1A). Previous studies using this protocol reported 0% (14) to 50–80% of arthritis incidence. (15) In our hands, no wild-type mice developed arthritis on this protocol (data not shown). We hypothesized that priming neutrophils by granulocyte colony-stimulating factor (G-CSF) would induce arthritis because G-CSF primes neutrophils to induce NETs (16) and exacerbates arthritis in CIA in DBA/1 mice. (17) We administered G-CSF for 4 consecutive days around the second CII injection (Figure 1A). Eleven out of 12 mice developed arthritis in G-CSF-treated mice while vehicle-treated mice did not (Figure 1B, Mice treated with G-CSF only did not develop arthritis, not shown.). G-CSF increased neutrophils in peripheral blood approximately two fold (Supplementary Figure 1A). G-CSF-treated mice showed higher serum levels of interleukin 6 (IL-6) on day 56 compared with vehicle-treated mice (Figure 1C, left panel). Because C57BL/6 mice produce IgG2c antibodies instead of IgG2a antibodies (9), we measured serum anti-CII IgG2c antibody along with anti-CII IgG antibody; there was no difference between vehicle- and G-CSF-treated mice (Figure 1C, center and right panels). We measured plasma levels of double-stranded DNA (dsDNA) and citrullinated histone H3 (H3Cit) as NET biomarkers on day 22. G-CSF-treated mice showed higher plasmas levels of NET markers compared with vehicle-treated mice (Figure 1D). When evaluated histopathologically, G-CSF-treated mice showed expansion of synovial tissue in the joint space while vehicle-treated mice exhibited no such expansion (HE stain, Figure 1E). Immunofluorescence microscopy revealed lesions positive for H3Cit and Ly6G (a mouse neutrophil marker) with DNA within the joint space and on the joint surface in

G-CSF-treated mice (Figure 1F). In contrast, vehicle-treated mice showed no lesion with H3Cit, Ly6G, and DNA. Finally, we sought to detect serum anti-H3Cit antibodies that exist in sera of RA patients as one of the anti-citrullinated protein antibodies (ACPA). (18) ELISA detected anti-native H3 antibodies and anti-H3Cit antibodies in serum in both G-CSF-treated and vehicle-treated mice (Supplementary Figure 1B). When the relative value of anti-H3Cit antibody to anti-native H3 antibody was calculated, G-CSF-treated mice showed a significantly higher anti-H3Cit antibody/anti-native H3 antibody ratio than the vehicle-treated mice (Figure 1G).

Based on data revealing enrichment of citrullinated histones, we sought to investigate the contribution of PAD4 in the process. We induced arthritis on littermate *Padi4*$^{+/+}$ and *Padi4*$^{-/-}$mice in the G-CSF-modified CIA model (Figure 2A). *Padi4* deficiency reduced arthritis incidence and severity (Figure 2B). *Padi4*$^{-/-}$ mice had reduced serum IL-6 and anti-CII IgG antibody on day 56, but comparable anti-CII IgG2c antibody levels (Figure 2C). *Padi4*$^{-/-}$ mice showed reduced increase of plasma dsDNA and H3Cit from day 20 to day 22 (Figure 2D). When evaluated by micro-computed tomography (micro-CT), fewer areas of the eroded surface of bones were observed in *Padi4*$^{-/-}$ mice (Figure 2E). HE staining of ankle joint inflammation (exudate and infiltrate) revealed *Padi4*$^{-/-}$ mice had less severe arthritis phenotype compared with *Padi4*$^{+/+}$ mice (Figure 2F). Immunofluorescence microscopy revealed lesions positive for H3Cit and Ly6G, and DNA within the joint space and on the bone surface in *Padi4*$^{+/+}$ mice but not in *Padi4*$^{-/-}$ mice (Figure 2G). Synovial tissue from *Padi4*$^{-/-}$ mice contained less MPO and H4Cit compared with that from *Padi4*$^{+/+}$ mice (Figure 2H). *Padi4*$^{-/-}$ mice also demonstrated a significantly lower anti-H3Cit antibody/anti-native H3 antibody ratio compared with *Padi4*$^{+/+}$ mice. (Figure 2I and Supplementary Figure 1C).

Fibroblasts are main constituents of synovial tissue of RA and their origin possibly consists of resident fibroblasts, pericytes, and mesenchymal stem cells. (19) Because fibroblast-like synoviocytes from RA patients express PAD4, (20) the origin of PAD4 is of interest. To address this issue, we used hematopoietic lineage-specific *Padi4* knockout mice (*Padi4*$^{Vav1Cre/+}$) in G-CSF-modified CIA. We confirmed that *Padi4*$^{Vav1Cre/+}$ had comparable *Padi4* RNA expression to *Padi4*$^{fl/fl}$ in organs (Supplementary Figure 2A). Additionally, we confirmed the *Padi4* protein expression in peripheral blood and the absence of *Padi4* protein expression in endothelial cells of the aorta (Supplementary Figure 2B) because *Vav1-iCre* is expressed in endothelial cells (12).

Padi4$^{Vav1Cre/+}$ mice had reduced arthritis incidence and severity compared with littermate *Padi4*$^{fl/fl}$ (Figure 3A). *Padi4*$^{Vav1Cre/+}$ mice had reduced serum IL-6; however, they had comparable serum levels of anti-CII IgG antibody and anti-CII IgG2c antibody on day 56 (Figure 3B). An increase in plasma dsDNA and H3Cit from day 20 to day 22 was detected in *Padi4*$^{fl/fl}$, but not in *Padi4*$^{Vav1Cre/+}$ mice (Figure 3C). *Padi4*$^{Vav1Cre/+}$ mice showed fewer areas of the eroded bone surface in the micro-CT compared with *Padi4*$^{fl/fl}$ (Figure 3D). Immunofluorescence microscopy revealed lesions positive for H3Cit and Ly6G, and DNA within the joint space and on the bone surface in *Padi4*$^{fl/fl}$ mice but not in *Padi4*$^{Vav1Cre/+}$ mice (Figure 3E). *Padi4*$^{Vav1Cre/+}$mice showed significantly reduced inflammation on the joint tissue, which was significant when semi-quantified (Figure 3F). Synovial tissue from

Padi4$^{Vav1Cre/+}$mice contained less MPO and H4Cit compared with that from *Padi4*$^{fl/fl}$ mice (Figure 3G). *Padi4*$^{Vav1Cre/+}$mice also displayed a lower anti-H3Cit antibody/anti-native H3 antibody ratio compared with Padi*4*$^{fl/fl}$ mice (Figure 3H and Supplementary Figure 1D).

DISCUSSION

There are conflicting data on the susceptibility of C57BL/6 mice to CIA ranging from no incidence (14) and less severity (21) to 50–80% incidence with mild severity. (15) Even in the well-known protocol, the authors described variability. (15) Pepsin used to prepare homemade collagen was reported to be strongly immunogenic and essential for arthritis development. (8) This may be one of the reasons for variability in incidence and severity in the model.

G-CSF-modified CIA model demonstrated reliably high arthritis incidence (90–100%) and severity suitable to compare different treatment groups. This model is considerate of animal welfare and acceptable to Institutional Animal Care and Use Committees (IACUCs). Additionally, in contrast to previous protocol of CIA on C57BL/6 mice using homemade collagen (15), our protocol uses commercially available collagen.

The presence of anti-CII antibody is thought to correlate with the development of arthritis. (7) However, G-CSF-treated mice presented comparable levels of anti-CII IgG and IgG2c with vehicle-treated mice. This suggests the production of anti-CII IgG is not sufficient to develop arthritis in G-CSF-modified CIA and other factors induced by G-CSF must be important.

Our G-CSF-modified CIA model has interesting features. The detection of H4Cit in synovial tissue is consistent with the detection of citrullinated H4 bound to ACPAs in RA synovial fluid. (22) Additionally, serum anti-H3Cit antibody mimics RA because it is detected in RA patients. (18) NETs are the likely origin of the citrullinated proteins in RA. (23) These features are helpful to study the relationship between citrullinated antigens and autoantibodies in RA.

The importance of G-CSF in arthritis has been shown in both clinical and basic studies. There are several case reports of G-CSF exacerbating RA (24) and a clinical study to demonstrate RA flares after filgrastim (G-CSF) administrations. (25) In a mouse study, injection of G-CSF exacerbated the severity of arthritis in CIA in DBA/1 mice. (17) Our results that the G-CSF-modified CIA causes arthritis accompanied with NET biomarkers in plasma and synovial tissue is a novel insight to consider the mechanism of effects of G-CSF on arthritis as well as the effects of G-CSF on neutrophil elevation. We show that the effect of G-CSF is primarily through PAD4 as *Padi4*$^{-/-}$ mice and *Padi4*$^{Vav1Cre/+}$ mice are significantly protected from G-CSF-modified CIA. G-CSF might promote neutrophil priming for NET formation and PAD4-dependent NETs could act as an adjuvant in arthritis. The remaining arthritis enhancing effect of G-CSF may be on blood cells other than neutrophils, other citrullinating enzymes, or non-citrullination processes.

This study has some limitations. We need to consider the influence of *Padi4* expressed not only in neutrophils but in monocyte and macrophages in the pathogenesis of this model.

Additionally, in our study, most sera from mice reacted with native H3 peptides more than H3Cit peptides, although ACPAs bind the citrullinated peptides much more than native peptides in RA patients. Therefore, there is only a limited pathological meaning of the anti-H3Cit antibody in this study, and controversies on detecting ACPAs in mouse arthritis models (26) should be considered. Although our G-CSF-modified CIA model has some features seen in human RA, we need to be aware of the differences of characteristics between human RA and this model. Another limitation is that we used only male mice in this study, whereas RA is seen predominantly in females. In a preliminary study, we found an arthritis incidence of 60% in female mice in this model (Supplementary Figure 3), thus likely the model could be adapted to females in the future.

In conclusion, we have demonstrated that G-CSF administration around the time of the booster collagen immunization significantly improves the CIA model in C57BL/6 mice with a greater than 90% incidence of arthritis, accompanied by markers of NET formation in plasma and synovial tissue. Importantly, this model addresses previous animal welfare standards concerns. Finally, we determined that hematopoietic cell-associated PAD4 promotes arthritis development in the G-CSF-modified CIA model. This model may prove to be of value in future RA research and the development of drugs targeting this disease.

Supplementary Material

Refer to Web version on PubMed Central for supplementary material.

Acknowledgements

We thank Dr. Bruce Ewenstein for his critical reading of this manuscript and Ms. Kristen Douthit for language editing and proofreading. This work was supported by Grant-in-Aid for JSPS Fellows (to ShF) and The Uehara Memorial Foundation (to ShF).

Funding

A grant from National Heart, Lung, and Blood Institute of the National Institutes of Health (grant R35 HL135765) to DDW

REFERENCES

1. Suzuki A, Yamada R, Chang X, Tokuhiro S, Sawada T, Suzuki M, et al. Functional haplotypes of PADI4, encoding citrullinating enzyme peptidylarginine deiminase 4, are associated with rheumatoid arthritis. Nat Genet 2003;34:395–402. [PubMed: 12833157]
2. Wang Y, Li M, Stadler S, Correll S, Li P, Wang D, et al. Histone hypercitrullination mediates chromatin decondensation and neutrophil extracellular trap formation. J Cell Biol 2009;184:205–213. [PubMed: 19153223]
3. Shelef MA, Sokolove J, Lahey LJ, Wagner CA, Sackmann EK, Warner TF, et al. Peptidylarginine deiminase 4 contributes to tumor necrosis factor alpha-induced inflammatory arthritis. Arthritis Rheumatol 2014;66:1482–1491. Available at: https://www.ncbi.nlm.nih.gov/pubmed/24497204. [PubMed: 24497204]
4. Suzuki A, Kochi Y, Shoda H, Seri Y, Fujio K, Sawada T, et al. Decreased severity of experimental autoimmune arthritis in peptidylarginine deiminase type 4 knockout mice. BMC Musculoskelet Disord 2016;17:205. Available at: https://www.ncbi.nlm.nih.gov/pubmed/27150598. [PubMed: 27150598]
5. Seri Y, Shoda H, Suzuki A, Matsumoto I, Sumida T, Fujio K, et al. Peptidylarginine deiminase type 4 deficiency reduced arthritis severity in a glucose-6-phosphate isomerase-induced arthritis model.

Sci Rep 2015;5:13041. Available at: https://www.ncbi.nlm.nih.gov/pubmed/26293116. [PubMed: 26293116]

6. Rohrbach AS, Hemmers S, Arandjelovic S, Corr M, Mowen KA. PAD4 is not essential for disease in the K/BxN murine autoantibody-mediated model of arthritis. Arthritis Res Ther 2012;14:R104. Available at: https://www.ncbi.nlm.nih.gov/pubmed/22551352. [PubMed: 22551352]
7. Brand DD, Latham KA, Rosloniec EF. Collagen-induced arthritis. Nat Protoc 2007;2:1269–1275. Available at: https://www.ncbi.nlm.nih.gov/pubmed/17546023. [PubMed: 17546023]
8. Bäcklund J, Li C, Jansson E, Carlsen S, Merky P, Nandakumar KS, et al. C57BL/6 mice need MHC class II Aq to develop collagen-induced arthritis dependent on autoreactive T cells. Ann Rheum Dis 2013;72:1225–1232. [PubMed: 23041839]
9. Campbell IK, Hamilton JA, Wicks IP. Collagen-induced arthritis in C57BL/6 (H-2b) mice: new insights into an important disease model of rheumatoid arthritis. Eur J Immunol 2000;30:1568–1575. Available at: https://onlinelibrary.wiley.com/doi/pdf/10.1002/1521-4141%28200006%2930%3A6%3C1568%3A%3AAID-IMMU1568%3E3.0.CO%3B2-R. [PubMed: 10898492]
10. Li P, Li M, Lindberg MR, Kennett MJ, Xiong N, Wang Y. PAD4 is essential for antibacterial innate immunity mediated by neutrophil extracellular traps. J Exp Med 2010;207:1853–1862. [PubMed: 20733033]
11. Hemmers S, Teijaro JR, Arandjelovic S, Mowen KA. PAD4-mediated neutrophil extracellular trap formation is not required for immunity against influenza infection. PLoS One 2011;6.
12. Joseph C, Quach JM, Walkley CR, Lane SW, Lo Celso C, Purton LE. Deciphering Hematopoietic Stem Cells in Their Niches: A Critical Appraisal of Genetic Models, Lineage Tracing, and Imaging Strategies. Cell Stem Cell 2013;13:520–533. Available at: 10.1016/j.stem.2013.10.010. [PubMed: 24209759]
13. Münzer P, Negro R, Fukui S, di Meglio L, Aymonnier K, Chu L, et al. NLRP3 Inflammasome Assembly in Neutrophils Is Supported by PAD4 and Promotes NETosis Under Sterile Conditions. Front Immunol 2021;12:1–16.
14. Stevanin M, Busso N, Chobaz V, Pigni M, Ghassem-Zadeh S, Zhang L, et al. CD11b regulates the Treg/Th17 balance in murine arthritis via IL-6. Eur J Immunol 2017;47:637–645. [PubMed: 28191643]
15. Inglis JJ, Simelyte E, McCann FE, Criado G, Williams RO. Protocol for the induction of arthritis in C57BL/6 mice. Nat Protoc 2008;3:612–618. Available at: https://www.ncbi.nlm.nih.gov/pubmed/18388943. [PubMed: 18388943]
16. Demers M, Wong SL, Martinod K, Gallant M, Cabral JE, Wang Y, et al. Priming of neutrophils toward NETosis promotes tumor growth. Oncoimmunology 2016;5:1–9.
17. Campbell IK, Rich MJ, Bischof RJ, Hamilton JA. The colony-stimulating factors and collagen-induced arthritis: exacerbation of disease by M-CSF and G-CSF and requirement for endogenous M-CSF. J Leukoc Biol 2000;68:144–150. Available at: https://jlb.onlinelibrary.wiley.com/doi/pdf/10.1189/jlb.68.1.144. [PubMed: 10914502]
18. Janssen KMJ, de Smit MJ, Withaar C, Brouwer E, van Winkelhoff AJ, Vissink A, et al. Autoantibodies against citrullinated histone H3 in rheumatoid arthritis and periodontitis patients. J Clin Periodontol 2017;44:577–584. [PubMed: 28370244]
19. Matsuo Y, Saito T, Yamamoto A, Kohsaka H. Origins of fibroblasts in rheumatoid synovial tissues: Implications from organ fibrotic models. Mod Rheumatol 2018;28:579–582. Available at: 10.1080/14397595.2017.1386837. [PubMed: 29067846]
20. Sorice M, Iannuccelli C, Manganelli V, Capozzi A, Alessandri C, Lococo E, et al. Autophagy generates citrullinated peptides in human synoviocytes: A possible trigger for anti-citrullinated peptide antibodies. Rheumatol (United Kingdom) 2016;55:1374–1385.
21. Svendsen P, Etzerodt A, Deleuran BW, Moestrup SK. Mouse CD163 deficiency strongly enhances experimental collagen-induced arthritis. Sci Rep 2020;10:1–12. Available at: 10.1038/s41598-020-69018-7. [PubMed: 31913322]
22. Meng X, Ezzati P, Smolik I, Bernstein CN, Hitchon CA, El-Gabalawy HS. Characterization of autoantigens targeted by anti-citrullinated protein antibodies in vivo: Prominent role for epitopes derived from histone 4 proteins. PLoS One 2016;11:1–14.

23. Khandpur R, Carmona-Rivera C, Vivekanandan-Giri A, Gizinski A, Yalavarthi S, Knight JS, et al. NETs are a source of citrullinated autoantigens and stimulate inflammatory responses in rheumatoid arthritis. Sci Transl Med 2013;5:178ra40. Available at: https://www.ncbi.nlm.nih.gov/pubmed/23536012.

24. Cornish AL, Campbell IK, McKenzie BS, Chatfield S, Wicks IP. G-CSF and GM-CSF as therapeutic targets in rheumatoid arthritis. Nat Rev Rheumatol 2009;5:554–559. [PubMed: 19798030]

25. Snowden JA, Biggs JC, Milliken ST, Fuller A, Staniforth D, Passuello F, et al. A randomised, blinded, placebo-controlled, dose escalation study of the tolerability and efficacy of filgrastim for haemopoietic stem cell mobilisation in patients with severe active rheumatoid arthritis. Bone Marrow Transplant 1998;22:1035–1041. [PubMed: 9877264]

26. Willis VC, Gizinski AM, Banda NK, Causey CP, Knuckley B, Cordova KN, et al. N-α-benzoyl-N5-(2-chloro-1-iminoethyl)-L-ornithine amide, a protein arginine deiminase inhibitor, reduces the severity of murine collagen-induced arthritis. J Immunol 2011:1001620.

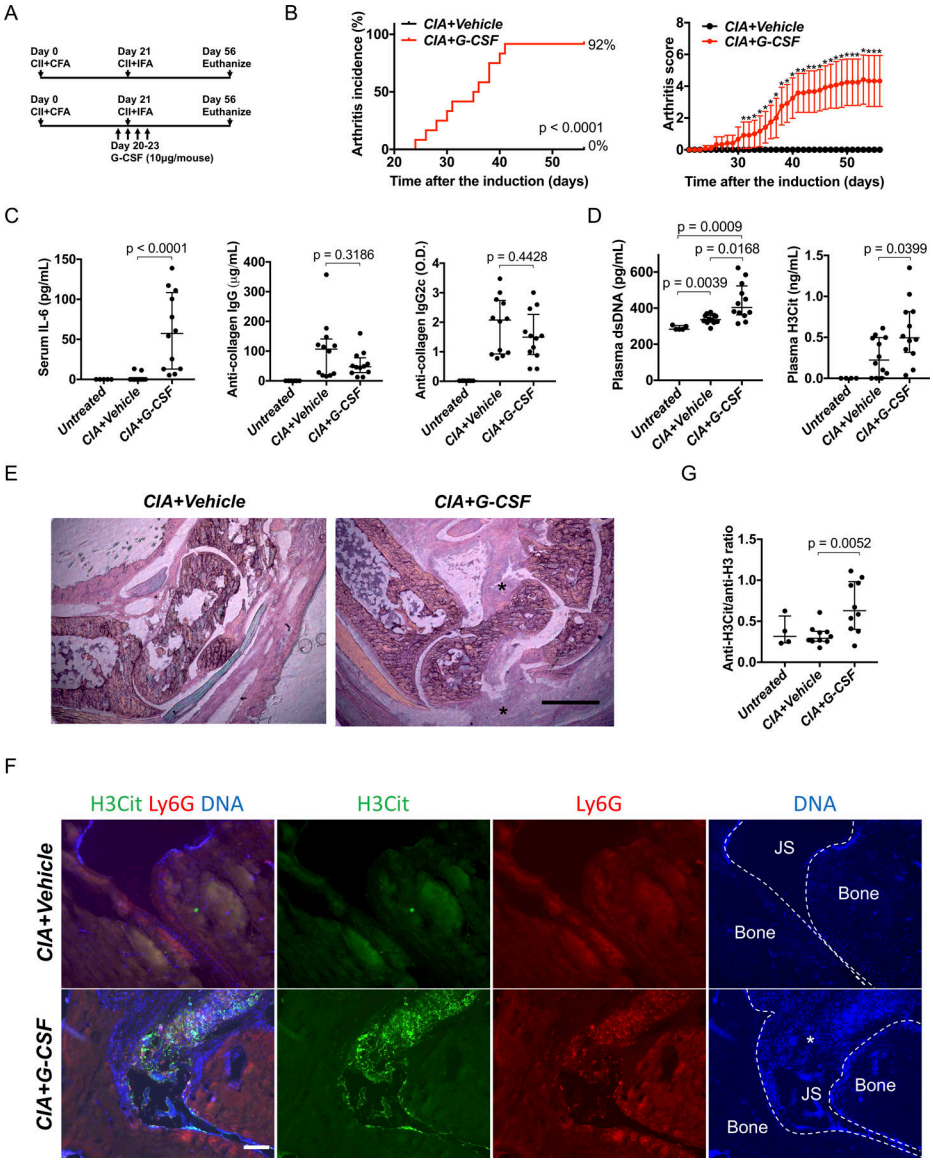

Figure 1. Exacerbation of collagen-induced arthritis on C57BL/6 strain by adding G-CSF injection

A: Injection schedule. B: Arthritis incidence (left) and severity (right) of vehicle-treated mice and G-CSF-treated mice (n=12:12). For arthritis severity, each line shows a mean with a 95% confidence interval. The severity scores on each day were used for Wilcoxon rank-sum test (*: $p < 0.05$). C: Serum IL-6 and serum anti-collagen IgG and IgG2c antibody on day 56 (n=12:12). D: Plasma levels of double stranded DNA (left) and citrullinated histone H3 (right) on day 22 (n=12:12). E: Representative images of hematoxylin-eosin (HE) stains using ankle joints (*: Expansion of synovial tissue seen only in G-CSF-treated mice, scale bar = 500μm). F: Representative images of immunostaining of Ly6G and H3Cit of ankle joints. (JS: Joint space, *: Synovial tissue, scale bar = 100μm) G: The comparison of ratio of anti-H3Cit antibody and anti-native H3 antibody calculated from ELISA optical density values in vehicle-treated mice and G-CSF-treated mice (n=10:10:4, vehicle-treated mice, G-CSF-treated mice, untreated mice).

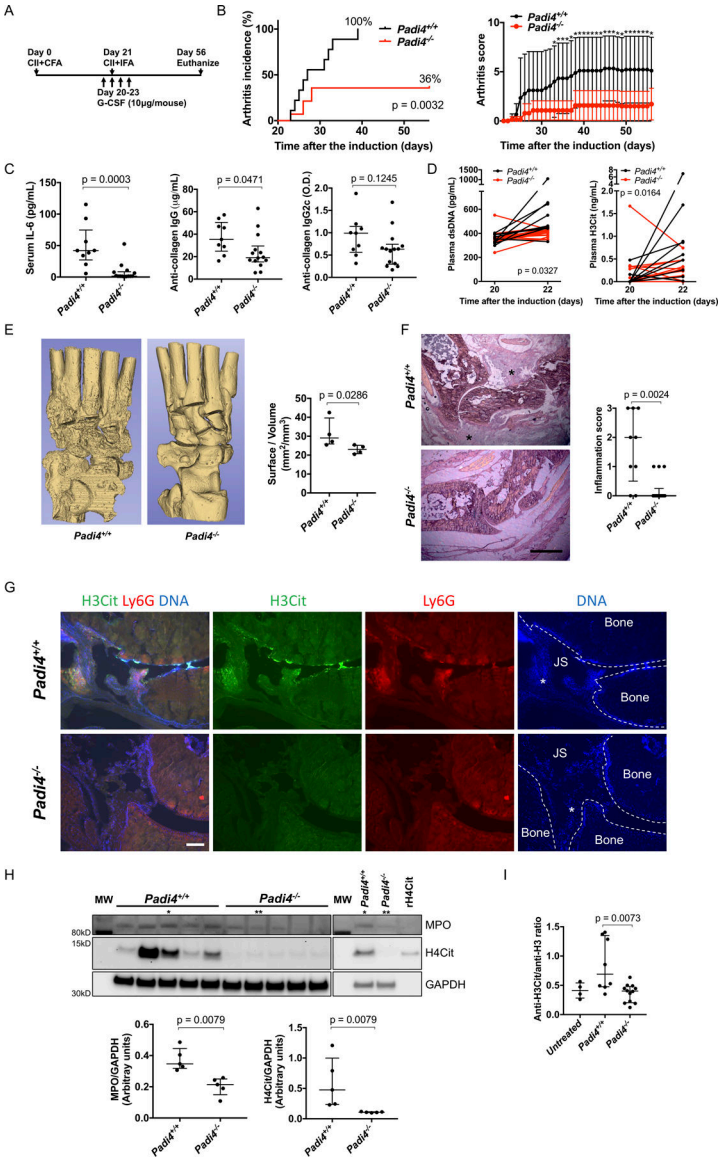

Figure 2. Comparison of *Padi4*$^{+/+}$ and littermate *Padi4*$^{-/-}$ in the G-CSF-modified CIA model

A: Injection schedule. B: Arthritis incidence (left) and severity (right) of *Padi4*$^{+/+}$ and *Padi4*$^{-/-}$ (n=9:14). For arthritis severity, each line shows a mean with a 95% confidence interval. The severity scores on each day were used for Wilcoxon rank-sum test (*: $p < 0.05$). C: Serum IL-6 and serum anti-collagen IgG and IgG2c antibody on day 56 (n=9:14). D: The changes of plasma levels of double stranded DNA (left) and citrullinated histone H3 (right) from day 20 to day 22 (n=9:14). The difference in change of value from day 20 to day 22 were used for Wilcoxon signed-rank test. E: Representative images of micro-CT of ankle joints (left) and quantification of eroded surface of joints (right, n=4:4). F: Representative images of HE stains using ankle joints and determination of inflammation in HE stains (left) by scale of 0 (no inflammation) to 3 (severe inflamed joint) depending on the number of inflammatory cells in the synovial cavity (exudate) and synovial tissue (infiltrate) determined blindly of genotype (right, n=9:14) (*: Proliferated synovial tissue.

scale bar = 500μm). G: Representative images of immunostaining of Ly6G and H3Cit of ankle joints (JS: Joint space, *: Synovial tissue, scale bar = 100μm). H: The blot of synovial tissue (n=5:5) for MPO, H4Cit, and GAPDH (upper, MW: molecular weight marker, rH4Cit: recombinant H4Cit as a positive control) and quantification by densitometry (lower, relative expression to GAPDH). * and ** indicates the same samples, respectively. I: The comparison of ratio of anti-H3Cit antibody and anti-native H3 antibody calculated from ELISA optical density values in *Padi4*$^{+/+}$ mice and *Padi4*$^{-/-}$ mice (n=8:12:4, *Padi4*$^{+/+}$mice, *Padi4*$^{-/-}$ mice, untreated mice).

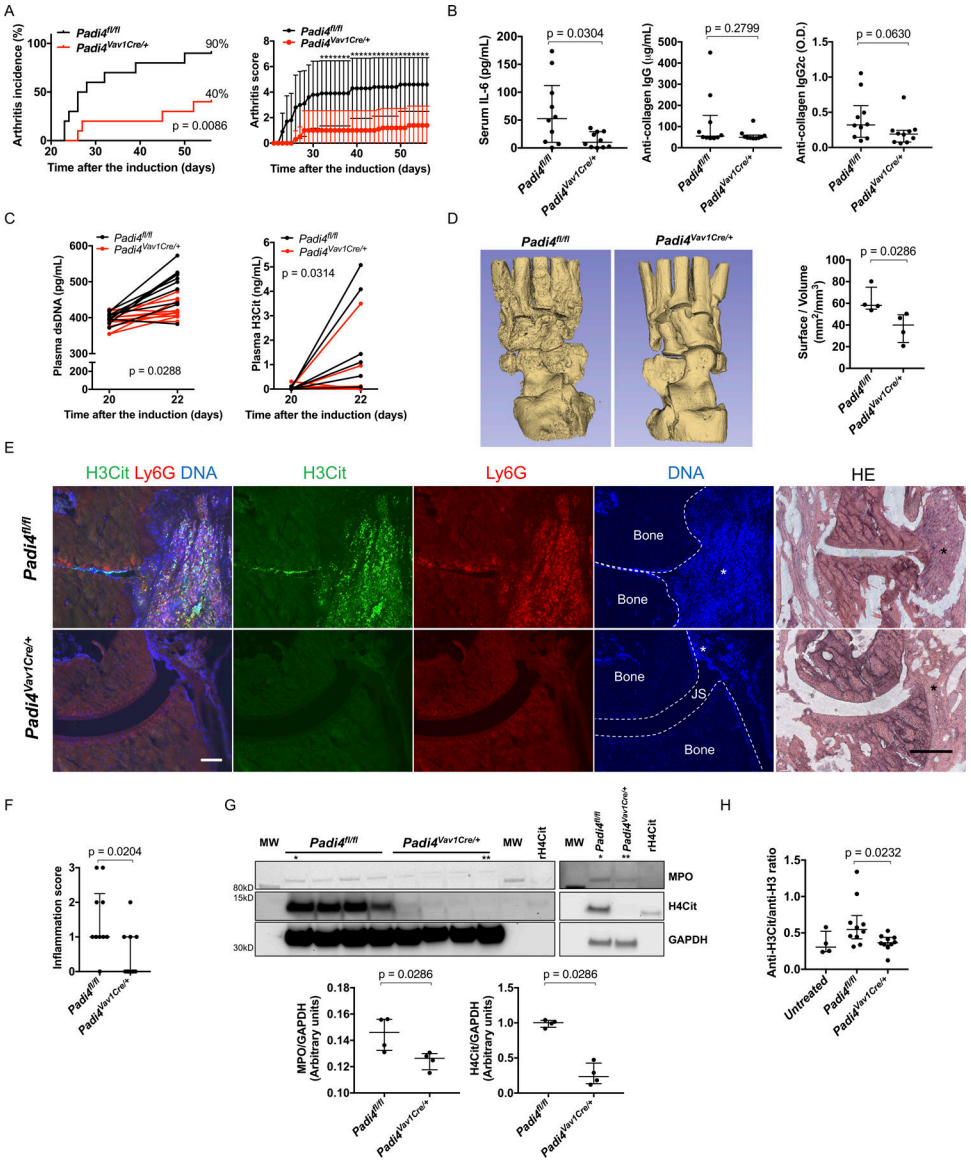

Figure 3. *Padi4*$^{fl/fl}$ and littermate *Padi4*$^{Vav1Cre/+}$ in G-CSF-modified CIA model

A: Arthritis incidence (left) and severity (right) of *Padi4*$^{fl/fl}$ and *Padi4*$^{Vav1Cre/+}$ (n=10:10) treated as in Figure 2A. For arthritis severity, each line shows a mean with a 95% confidence interval. The severity scores on each day were used for Wilcoxon rank-sum test (*: $p < 0.05$). B: Serum IL-6 and serum anti-collagen IgG and IgG2c antibody on day 56 (n=10:10). C: The changes of plasma levels of double stranded DNA (left) and citrullinated histone H3 (right) from day 20 to day 22 (n=10:10). The difference in change of value from day 20 to day 22 were used for Wilcoxon signed-rank test. D: Representative images of micro-CT of ankle joints (left) and quantification of eroded surface of joints (right, n=4:4). E: Representative images of immunostaining of Ly6G and H3Cit and HE stains using ankle joints (JS: Joint space, *: Proliferated synovial tissue, scale bar = 100μm). F: The determination of inflammation in HE stains by scale of 0 (no inflammation) to 3 (severe inflamed joint) depending on the number of inflammatory cells in the synovial cavity

(exudate) and synovial tissue (infiltrate) determined blindly of genotype (n=10:10). G: The blot of synovial tissue (n=4:4) for MPO, H4Cit, and GAPDH (upper, MW: molecular weight marker, rH4Cit: recombinant H4Cit as a positive control) and quantification by densitometry (lower, relative expression to GAPDH). * and ** indicates the same samples, respectively. H: The comparison of ratio of anti-H3Cit antibody and anti-native H3 antibody calculated from ELISA optical density values in *Padi4*$^{fl/fl}$ mice and *Padi4*$^{Vav1Cre/+}$ mice (n=10:10:4, *Padi4*$^{fl/fl}$ mice, *Padi4*$^{Vav1Cre/+}$ mice, untreated mice).